

**COMPARISON OF ATLAS TILECAL MODULE#8  
HIGH PRECISION METROLOGY RESULTS BY  
JINR – LASER AND CERN – PHOTOGRAMMETRIC METHODS**

*V.Batusov<sup>1</sup>, J.Budagov<sup>1</sup>, J.C.Gayde<sup>2</sup>, J.Khubua<sup>1</sup>, C. Lasseur<sup>2</sup>, M.Lyablin<sup>1</sup>,  
L.Miralles Verge<sup>2</sup>, M.Nessi<sup>2</sup>, N.Rusakovich<sup>1</sup>, A.Sissakian<sup>1</sup>, N.Topiline<sup>1</sup>*

<sup>1</sup> JINR, Dubna; <sup>2</sup> CERN, Geneva; <sup>3</sup> IFAE, Barcelona

### **Abstract**

The high precision assembly of a large experimental set-ups is of a principal necessity for the successful execution of the forthcoming LHC research program in the TeV-beams. The creation of an adequate Survey&Control METROLOGY METHODS are an essential part of the detector construction scenario. This work contains the dimension measurement data for ATLAS hadron calorimeter MODULE#8 (6m long, 22tons) which were obtained by LASER and by PHOTOGRAMMETRY methods. The comparative data analysis demonstrates the measurements agreement within  $\pm 70\mu\text{m}$ . It means these two clearly independent methods can be combined and lead to the rise of a new generation engineering culture: high precision metrology when precision assembly of large scale massive objects.

### **1. Introduction**

The ATLAS hadron Tile Calorimeter is composed [1] of one barrel and two extended barrels (Fig.1). Radially the Tile Calorimeter extends from an inner 2.8 m radius to an outer 4.25 m radius. Azimuthally, the BARREL and Extended BARRELS are divided into 64 MODULES.

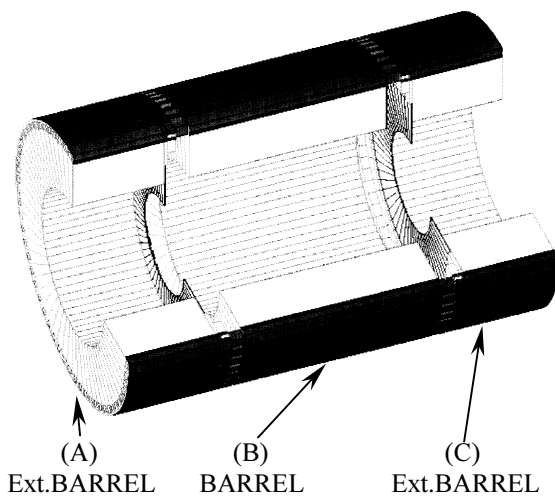


*Fig. 1 The Tile calorimeter: BARREL and two Extended BARREL*

Dubna began mass production of BARREL MODULES in April, 1999. *Appendix#1* gives BARREL MODULE assembly scheme. To guarantee very high MODULES assembly precision, we proposed, developed and practically applied the unique new Laser Control System [2,3]. The Laser Control System instrumentation and brief method description see in *Appendix#2*.

In January 2000 the JINR and CERN groups measured the ATLAS Tile Calorimeter MODULE#8 dimensions by the LASER and PHOTOGRAMMETRIC methods at CERN.



The photogrammetric instrumentation and method are documented in *Appendix#3*

During these measurements the MODULE was kept at the same position which allowed one to obtain the data for comparison of both methods. Clearly, these measurement methods are fully independent.

It must be also noted that the MODULE#8 was measured by standard surveying method using theodolites for industrial 3D metrology before the application of the photogrammetric method; the standard deviation (1 sigma) according to the DIN 18723 norm is given to 0.15 mgon (0.5 ″) for both horizontal and vertical angles measurements. See the results in <http://edms.cern.ch/document/309991/1>

A small reference network was arranged around the MODULE in such a way that the theodolites sights were nearly parallel to the faces: therefore, the accuracy on the coordinate perpendicular to the face was given by the high precision of the angle measurements.

The survey results for both of the geometric methods, and the comparisons have been documented in the reports noted in *Appendix#4*

In two sets of measurements (PHOTO and LASER) we had the following 4 measurement lines (common for both methods) on the MODULE surface [3] (see Fig. 2):

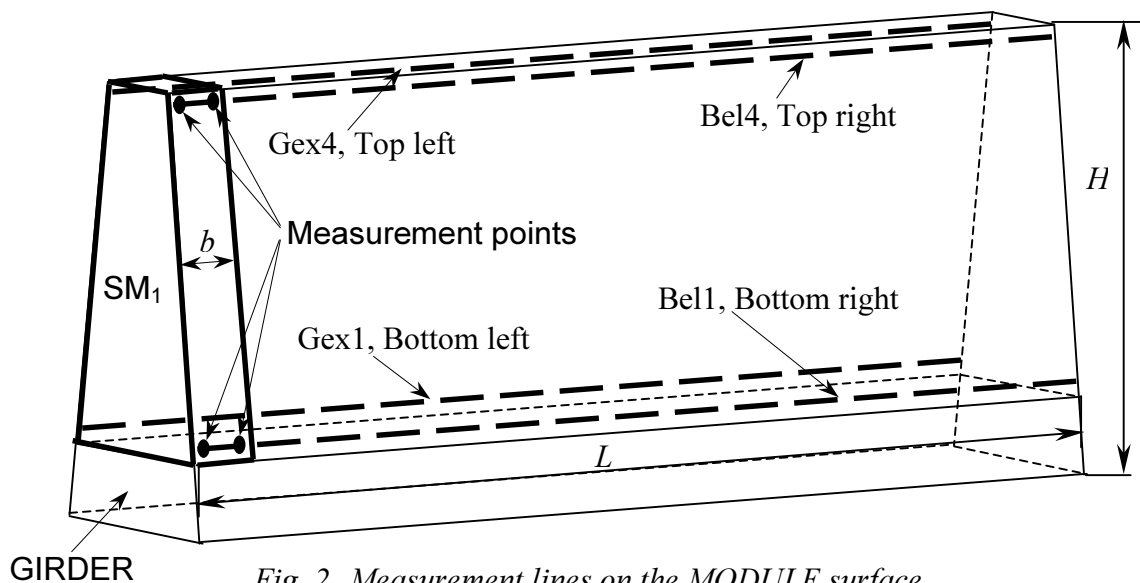


Fig. 2 Measurement lines on the MODULE surface.

- Bottom left<sup>1)</sup> of the LASER method coincides with the bottom left line Gex1<sup>2)</sup> of the PHOTOGRAMMETRIC method;
- Top left coincides with Gex4;
- Bottom right<sup>1)</sup> coincides with Bel1<sup>3)</sup>;
- Top right coincides with Bel4;

<sup>1)</sup> The left (right) side of the MODULE is the side on the left (right) of the observer looking from the SM1 along the MODULE

<sup>2)</sup> Direction to the town Gex

<sup>3)</sup> Direction to the town Bellegarde

Comparison was made only along these lines.

In the PHOTOGRAMMETRIC method the measurement points were located (Fig. 2) on the submodule (SM) surface at a distance of  $1/4 \times b$  from the submodule edge ( $b$ – is the submodule width). The MODULE height  $H=1940$  mm and its length is  $L=5600$ mm.

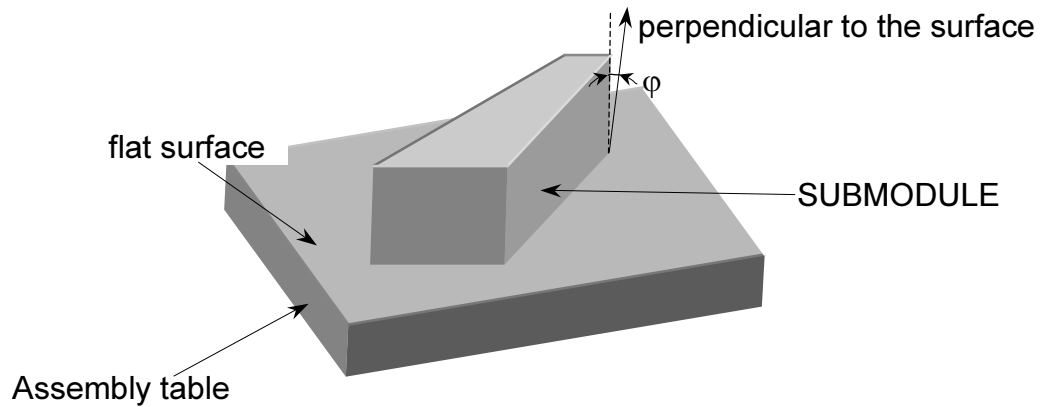


*Fig.3 Definition of submodule maximal twist angle  $\varphi$*

In the LASER method the measurement points were located on the submodule edges. This location of the measurement points was motivated by the presence of the submodule twist angle  $\varphi$  (Fig.3) and, consequently, only at such a positioning one can detect (observe) the parts, going farthest beyond the limits of the MODULE. We note that the Top-lines data will expectedly demonstrate the largest discrepancies in comparison to the Bottom-lines data as it is in the narrow part of the submodule that one observes the maximal twist angles  $\varphi$  reaching the value of  $10^{-4}$  rad.

## 2. **Coordinate Systems (CS)**

### *Requirements to the CS*

When choosing CS it seems natural to fix it to some element of the MODULE. It should be taken into account that the dimensions and shape (form) of such element (surface, edge) may differ from its shop-drawing dimensions (non-flat, not straight-lined, twisted etc).

As a result, systematic errors may arise and deteriorate final measurement precision.

In this sense it seems essential that the systematic error should be at worst comparable with the measurement precision. Otherwise the choice of the CS can give a distorted idea of the MODULES measured.

### *CS of JINR Laser method*

The choice of the CS is determined by the Dubna technology of the MODULE assembly [1]. The center “ $O_L$ ” of the CS is chosen in the middle of the bottom edge of the girder base surface from the side of submodule #1 (see Fig.4).

- The  $Y_L$  axis goes along the line, which connects the point  $O_L$ , and point “N”, which is the middle (center) of the bottom base of the girder at the side of submodule #19.
- The  $Z_L$  axis goes along the line connecting the point  $O_L$  and point “M” in the middle of the edge of the narrow part of the special submodule from the side of the endplate.
- The  $X_L$  axis is perpendicular to the  $Z_L$  and  $Y_L$  axes.

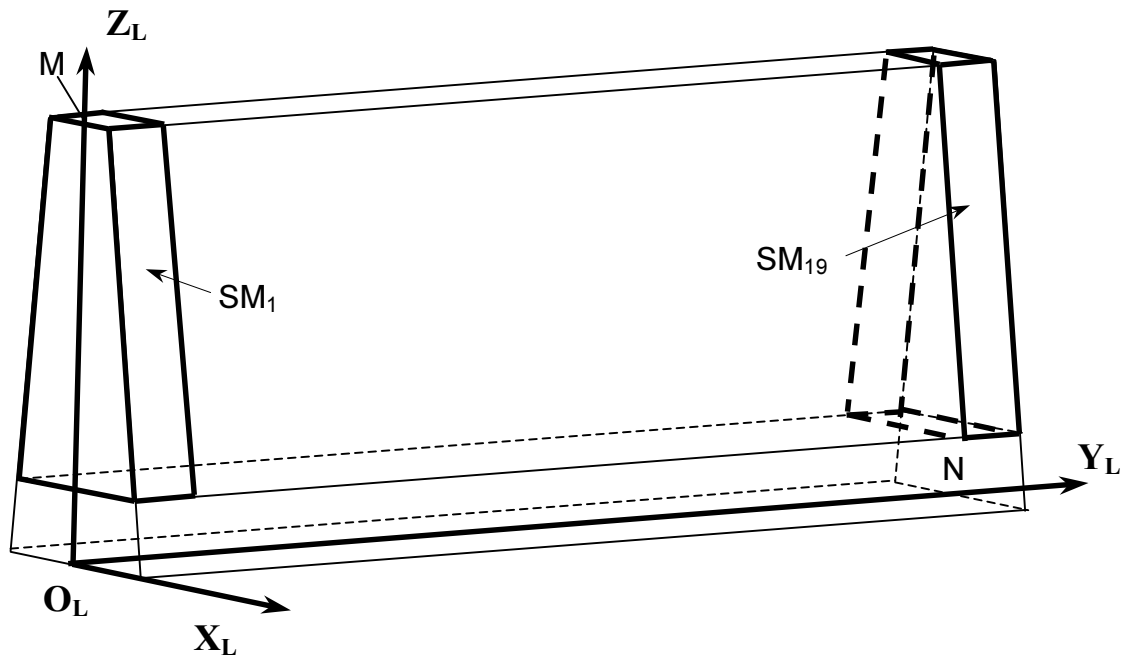


*Fig.4 Coordinate System of the Laser method*

### *CS of the CERN photogrammetric method and measured points*

The four extreme corners of the girder were measured and set in the same horizontal plane within a max – min of 0.1 mm with using a precise optical level (precision of a direct measurement : 30 microns, then precision of a vertical differences between 2 corners : 42 microns).

The distances between the corners were measured within an accuracy of 0.1 mm using a precise electro-optical distancemeter associated to a metrological class theodolite as mentioned above. Then the coordinate system for the photogrammetry is referred to the plane of the girder, set horizontal, and to the four corners of the girder, altogether within 0.1 mm; that margin value is referred to the procedure of setting the four extreme corners of the girder horizontal by using a precise optical level.

The Coordinate center “ $O_p$ ” is the centroid of the four bottom corners of the girder (Fig. 5).

- The  $Y_P$  axis is in the mean plane of the four corners and parallel to the girder longitudinal axis
- The  $Z_P$  axis is perpendicular to the mean plane of the four corners
- The  $X_P$  axis is in the mean plane of the four corners at the origin and perpendicular to the  $Y_P$  axis
- The plane  $X_P O_P Y_P$  is horizontal within 0.1 mm i.e 0.02 mrad as a longitudinal tilt angle and 0.2 mrad as a transversal tilt angle; the  $Z_P$  axis is vertical within the same accuracy along the two angular components.
- Despite the accuracy of the photogrammetric process, within 50 microns spatially at 1 sigma, and in order to include the uncertainty on the definition of the CS, all the results documented in the reports were given within 100 microns accuracy.

In fact the four corners, measured by standart precise level and metrological class theodolite, were also measured by photogrammetry so that the coordinates given by that method were directly expressed in the CS as described above.

Each submodule was equipped by 16 coded retroreflective targets (3 cm \* 3 cm), 8 on each side and arranged by 2 at 4 levels quoted respectively at 0.35 m, 0.88 m, 1.44 m and 1.77 m from the reference mean plane of the four corners measured and set horizontal as described above. That regular arrangement permitted to calculate the thickness of the module at each level, to give the median plane at each level i.e. the misalignment with respect to the reference axis of the girder and then the spatial banana shape of the entire MODULE. Finally there were 152 points measured on each side for the definition of the MODULE envelope and its geometrical parameters, all referred to the girder as defined before.

In addition to the these parameters, the best fit plane was calculated for each side, the differences for each point to the mean plane also so that the max and min values were identified easily. The wedge angle was calculated for the entire MODULE and could be extracted for each submodule.

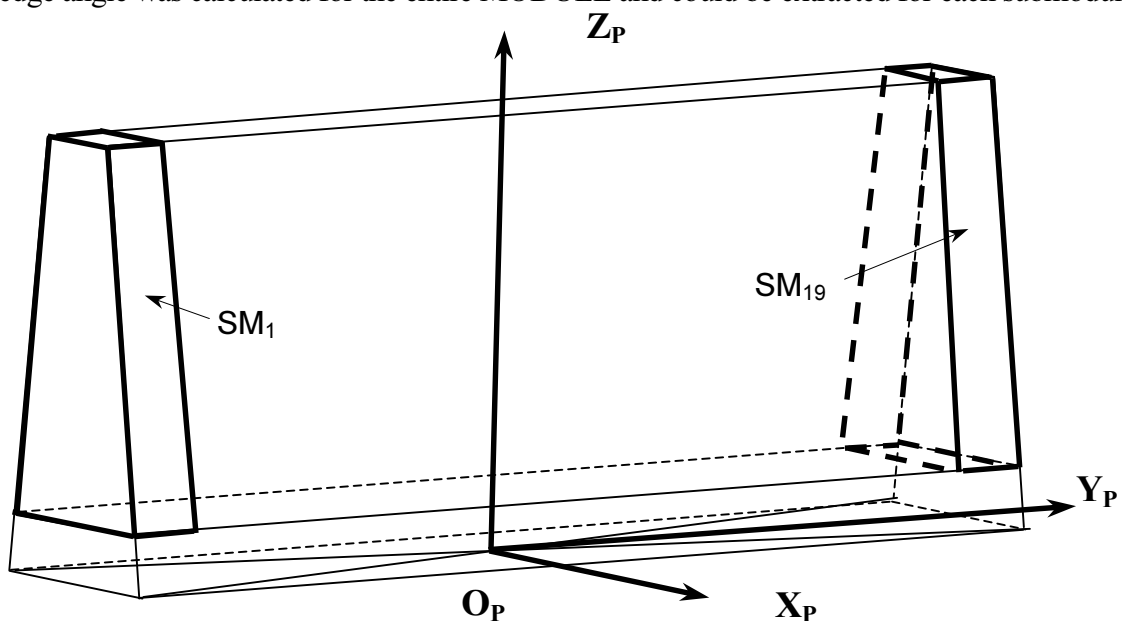


*Fig. 5 Coordinate System of the photogrammetric method*

*Comments on the CS of the CERN PHOTOGRAMMETRIC method*

1. The girder may have the following (compared with the drawing) distortions measured at JINR by the Dubna Survey group:

- A) The girder may have the “twist” angle  $\varphi_G$  (Fig. 6); we measured this angle by the MINILEVEL:  $\varphi_G=10^{-4}$  rad.

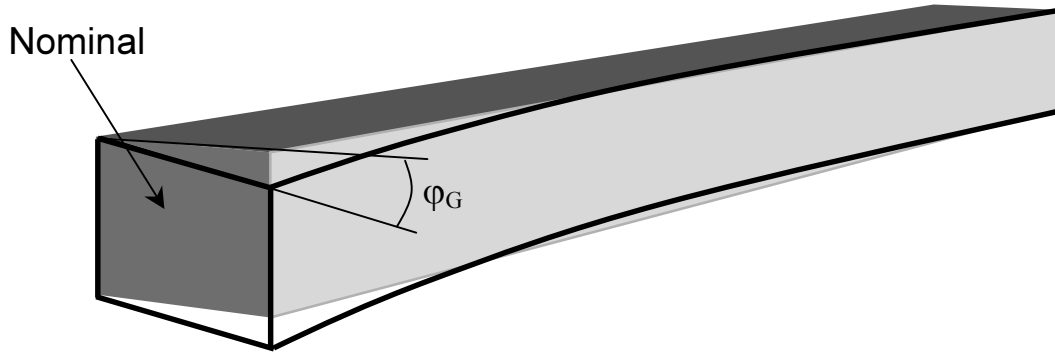


*Fig. 6 “Twist” of the girder*

- B) The girder may have a banana shape (Fig. 7).

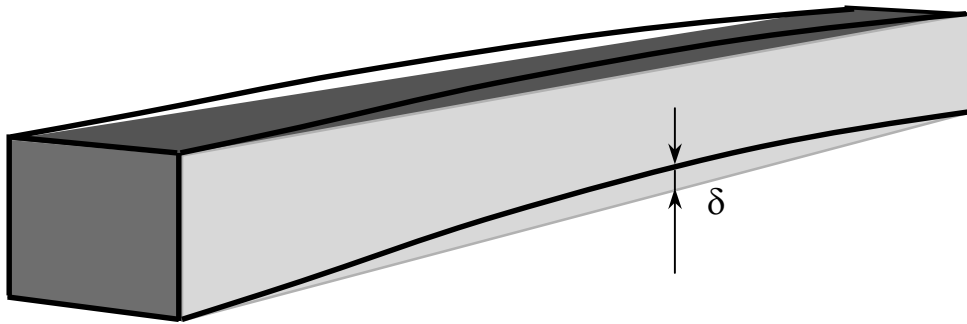


*Fig. 7 Sagging (“banana”) of the girder*

Sagging may reach a value of  $\delta=0.6$  MM. As the girder bottom surface is not flat, the possible final effect is that the CS can be not orthogonal! It seems to us that this is practically impossible to take into account this effect as one cannot determine the shape of the bottom girder base (down plane) for the already assembled MODULE.

2. The lines of the long side edges of the bottom girder base are not straight-lined and sagging may reach  $\delta_{MAX}=0.6$  MM (Fig. 8).

The difference  $\delta_1 \neq \delta_2$  may lead to the asymmetric location of the coordinate center  $O_P$

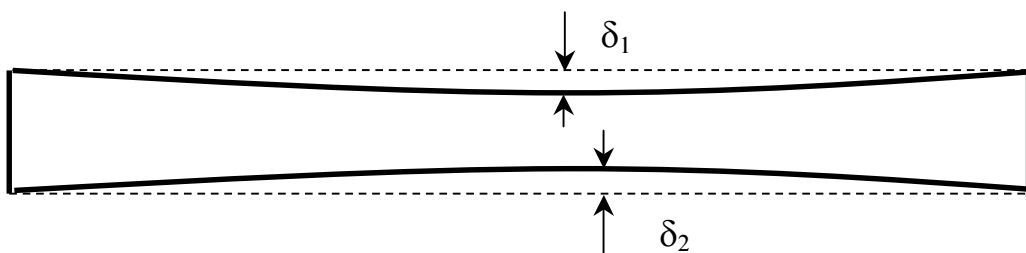


*Fig. 8 Sagging of side edges of the girder bottom base*

3. As was already said, the girder arrived from Romania with some residual “twist” along the longitudinal axis and this twist may reach  $\varphi_G = \pm 2 \cdot 10^{-4}$  rad (our data for girder #12). One can measure the twist before the MODULE is assembled, or before submodules are positioned. After the MODULE is fully assembled, the twist amplitude will change in an uncontrolled manner. If, however, one assumes that this change is insignificant, one can conclude that the vertical axis of the girder is oriented at the angle  $\varphi_K = \pm 2 \cdot 10^{-4}$  rad relative to the vertical axis of the submodule (see Fig. 9). This effect (twisting of the girder) will finally influence the photogrammetric data: the measured “distance” (distance from the ideal MODULE surface to the nearest points of the real MODULE) will be bigger on one side of the MODULE and smaller on the other. In other words, the pseudo-worsening of the photogrammetric measurement data will take place.

It must be noted at that stage that one advantage of the photogrammetric method is to give a full complete geometrical envelope of the MODULE referred to a proper reference attached to the object itself, namely the girder which is the real backbone of the assembly of the MODULES. See the section on the measured points.

***Comments on the CS of the JINR LASER method***

Because of “item 3” (see above) the systematic error will appear in determination of the coordinates of the Bottom-line along the X axis. The magnitude of this error (for maximal observed  $\theta = \pm 2 \cdot 10^{-4}$  rad of the girder twist) will be  $\Delta = 60 \mu\text{m}$ , which is compatible with the measurement precision. Note that following the MODULE assembling technology, the girder is to be positioned on the base unit in such a way that its “twist” must be symmetric about horizontal line (Fig. 9).

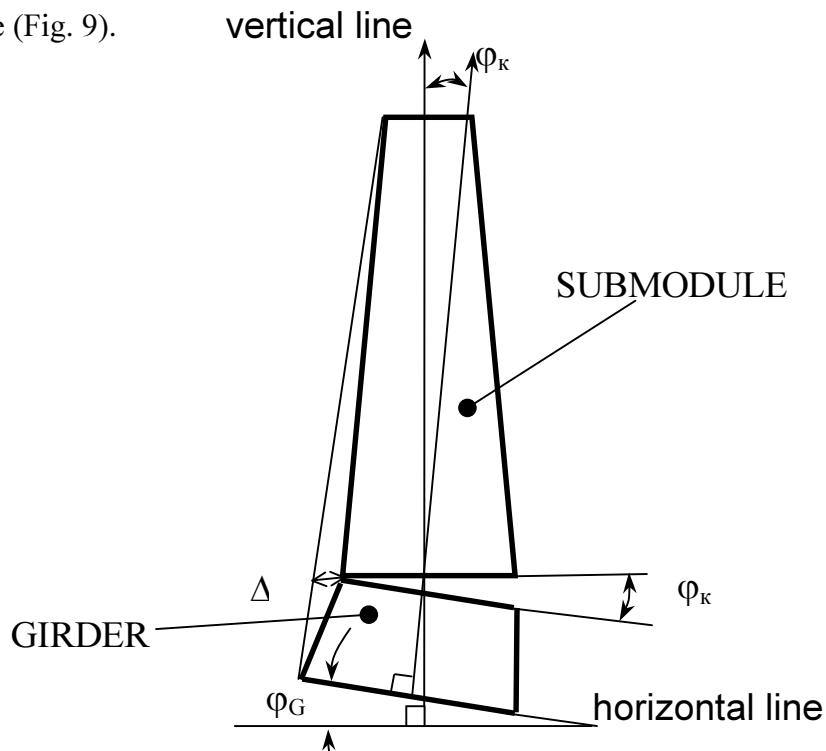


Fig. 9 Relative position of the submodule and of the “twisted” girder

### 3. Data presentation.

The results of both methods are presented in the form of the table (see *Appendix#5*) of deviation of the measured points from the surface of the Nominal MODULE (Fig.10).

- Top size “A” is the size that coincides with the width of the narrow part of the master plates in the indicated place.

- The “1-2-3-4” contour coincides with contour of the master plates.

For the Laser method the dimensions of the nominal MODULE are:

A = 223.31 mm, - top (narrow) base;

B = 408.80 mm, - bottom (wide) base;

C = 1942 mm, - height;

L = 5600 mm, - length;

B' = 414.16 mm, - theoretical dimension derivable as a result of master plates imaginary extension on the 1942 mm height.

The nominal MODULE must be positioned in such a way that positive maximal deviations of both sides of MODULE became equal (sort of "simmetrization" of the positive deviations).

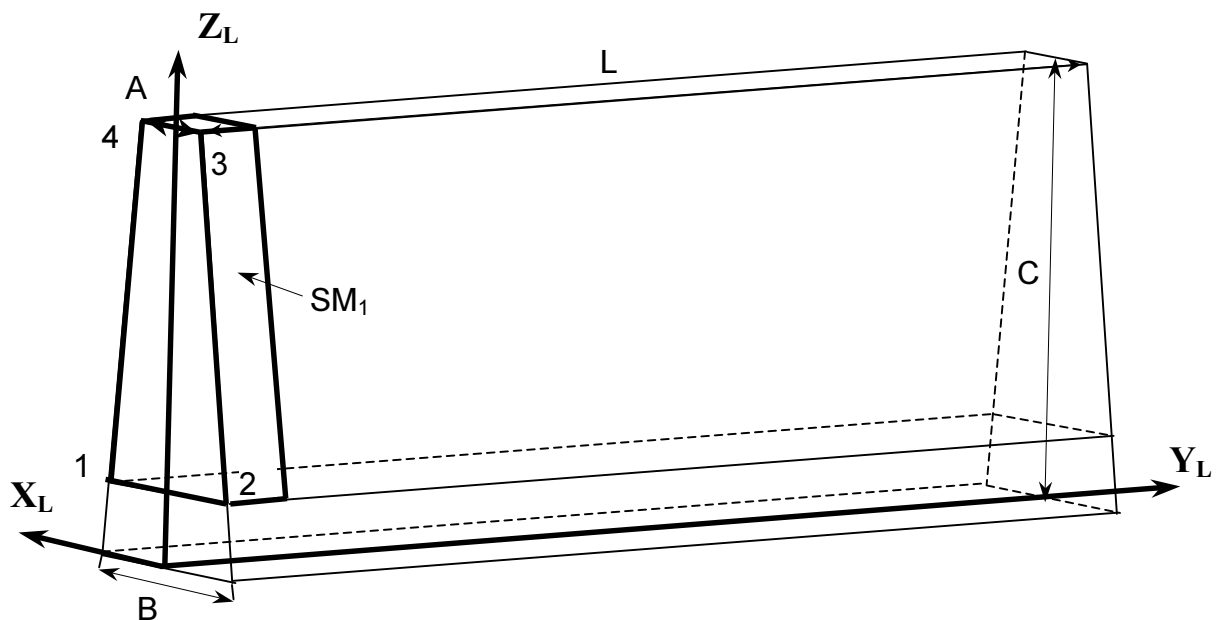


*Fig. 10 Position of the Nominal MODULE in the Laser method Coordinate System*



## 4. Results of comparison

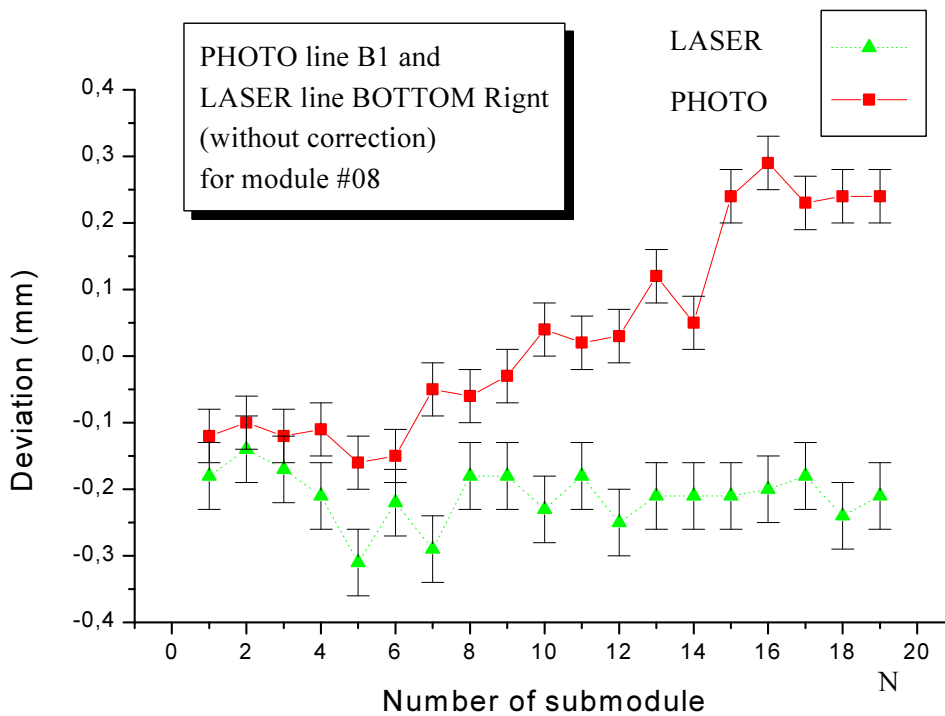
### *Transformation of the Laser data to the photogrammetric data*

Fig. 11 presents nontransformed (primary) data for both methods (see item 1 of our comments on the CS of the photogrammetric method). Recall that the twist angle  $\varphi = \pm 2 \cdot 10^{-4}$  was determined for the girder of MODULE #10.

We find it rather logical to assume that the MODULE #8 twist is also  $\varphi \approx \pm 10^{-4}$ .

If so, one may expect that (attention!) MODULE #8 in the Laser measurements will be turned as a whole by an angle of  $\approx 10^{-4}$  rad as compared with the photogrammetric method.

This assumption is confirmed by the measurement data disposition Fig. 11. Indeed, if one turns the Laser set of measurements by an angle  $\theta_0 = 0.8 \cdot 10^{-4}$  along the Y axis the Laser data set practically coincides with the photogrammetric series.



*Fig.11 Line Bell measurements data by the Photogrammetric and Laser Bottom-right methods with no correction applied*

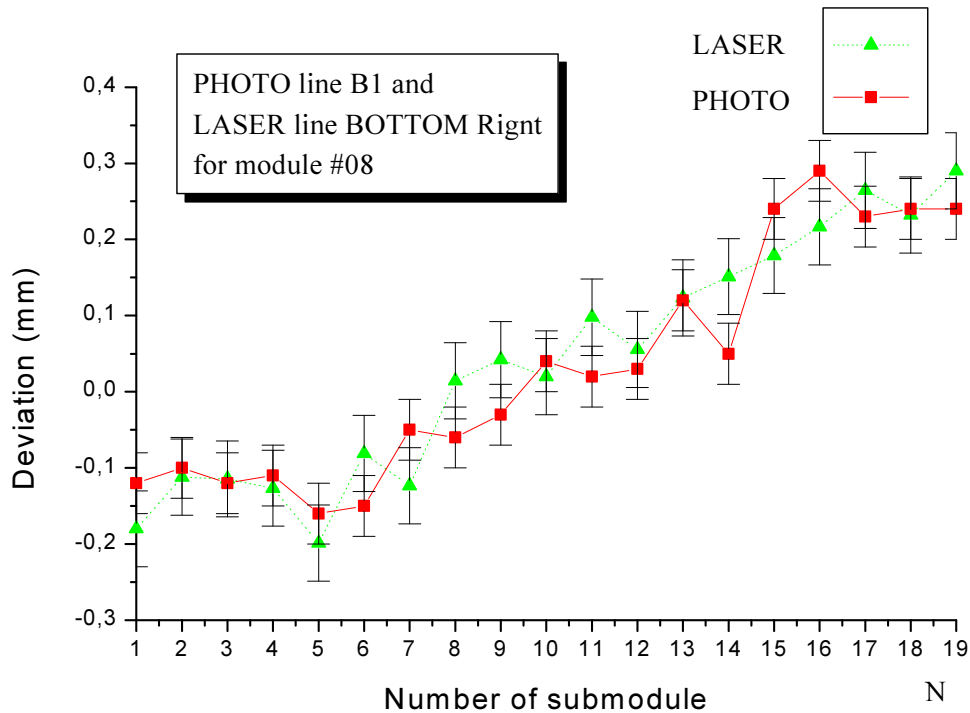


Fig.12 Line Bell measurements data by the Photogrammetric and Laser Bottom-right methods after correction (turn by  $0.8 \times 10^{-4}$  rad)

One more disagreement between the data of both methods is clearly visible (see *Appendix #5*). The envelope top overall size chosen in the photogrammetric method (the A-value in Fig. 10) is 0.3 mm narrower than in the LASER method (see *Appendix #5*).

Direct caliper measurements of the outer dimensions of the master plates on the narrow part (these are the dimensions which determine the envelope top overall dimension) indicate that the master plates were manufactured about 0.3-0.4 mm smaller than the nominal size. It is in favor of the overall dimension chosen in the LASER method (see item 3).

To reach the most complete data coincidence we turned the LASER data by an angle  $\theta_0 = 0.8 \times 10^{-4}$  rad with respect to Z-axis and also made the overall dimension noncontradicting in both methods (Fig. 12). The value obtained for  $\theta_0$  agrees with the above estimate correction angle  $\approx 10^{-4}$  rad.

In figs. 11-12 the data analysis shows good agreement for the shapes of the curves too. *Appendix#6* represents a very full data set and shows that after “turning” correction (see above) LASER&PHOTOGRAMMETRIC results are in agreement with the precision quoted on the histogram. The  $\sigma$ -value of the distribution of  $D_L - D_P$  differences (or “distances”), measured by the LASER and methods is:

$\sigma_b = 65 \mu\text{m}$  for Bottom-lines;

$\sigma_t = 90 \mu\text{m}$  for Top- lines.

As was mentioned in the introduction, the  $\sigma_t$  value for the TOP lines always turn out to be larger than  $\sigma_b$ .

All the above results confirm the quoted measurement precision. The coincidence of the shapes of the distributions of the results obtained by both methods is enough to state that both methods are close in precisions.

## 5. Conclusion.

Measurements performed by both methods indicate that MODULE #8 is within tolerance (0.6 mm from the nominal size).

Impressive coincidence of both Laser and Photo fully independent methods has been achieved by applying two corrections:

- Turning of the Laser method data by an angle  $\theta_0 = 0.8 \cdot 10^{-4}$  rad with respect to the Z axis;
- Correction of the Nominal MODULE width in the Nominal MODULE top part (see item 3, size “A”) chosen in the Photo method; this correction is based on direct measurements of size “A”.

So the results of measuring the “MODULE geometry” by both methods coincide with an accuracy of about  $(\sigma_b + \sigma_t)/2 \approx 80 \mu\text{m}$ .

All the above-said allows one to conclude that, as we understand:

it seems very important to use BOTH METHODS (they are INDEPENDENT) for fulfilling such a complex technical task as the precision assembly of the BARREL HADRON CALORIMETER and a much more difficult task like final assembly of all ATLAS systems in the near future.

The joining of the JINR and CERN groups’ efforts might lead to the rise of ENGINEERING CULTURE of a NEW GENERATION: high-precision metrology when precision assembling of large-scale massive objects.

## Acknowledgements

The CERN team would like to express their thanks to the JINR team for having initiated that study and incorporated the photogrammetry concepts and results, specially Professors Julian Budagov and Djemal Khubua. The CERN team is grateful for Nikolai Topilin for helped with technical documented development.

Some other persons from the CERN team participated to the regular measurements of the tile MODULES : Katia Nummiaro, Dirk Mergelkuhl, Jean-Frédéric Fuchs for the photogrammetric parts – measurements, analysis and report - Jean Noel Joux and André Froton for the geometrical preparatory works.

The JINR team thanks INTAS for the financial support of the JINR team work with grant INTAS-CERN#288.

The JINR team thanks Yu.Lomakin for his very large contribution on all stages of the MODULE assembly at JINR. We are grateful to V.Romanov, M.Nazarenko, S.Tokar and A.Shchelchikov for their help in various stages on assembly technology development, accumulated data passportization, high precision measurements tooling delivery, solving of a numerous custom&transport problems.

### **References**

- [1]. A. Airapetian et al; CERN/LHCC/ 96-42(1996).
- [2]. Metrological inspection of MODULES of hardon calorimeter for ATLAS detector.  
B.A. Alikov et al. Tile Cal inter Nat Note # 79,1997.
- [3]. V. Batusov, et al; "Particles and Nuclei, Letters", JINR, Dubna 2 (105) 33(2001).

**BARREL MODULE ASSEMBLY SCHEME**

The ATLAS Barrel Hadron Tile Calorimeter MODULE production is a multistage process. A MODULE consists of the following main elements: 1 girder, 19 submodules, two end plates and two front-plates (Fig.13). Each of the above elements is supposed to be produced within the required geometrical tolerances. The most stringent requirement on the MODULE assembly is the planarity of its side surface (1.9 m x 5.6 m), this to allow a correct stacking of the cylinder during the final assembly

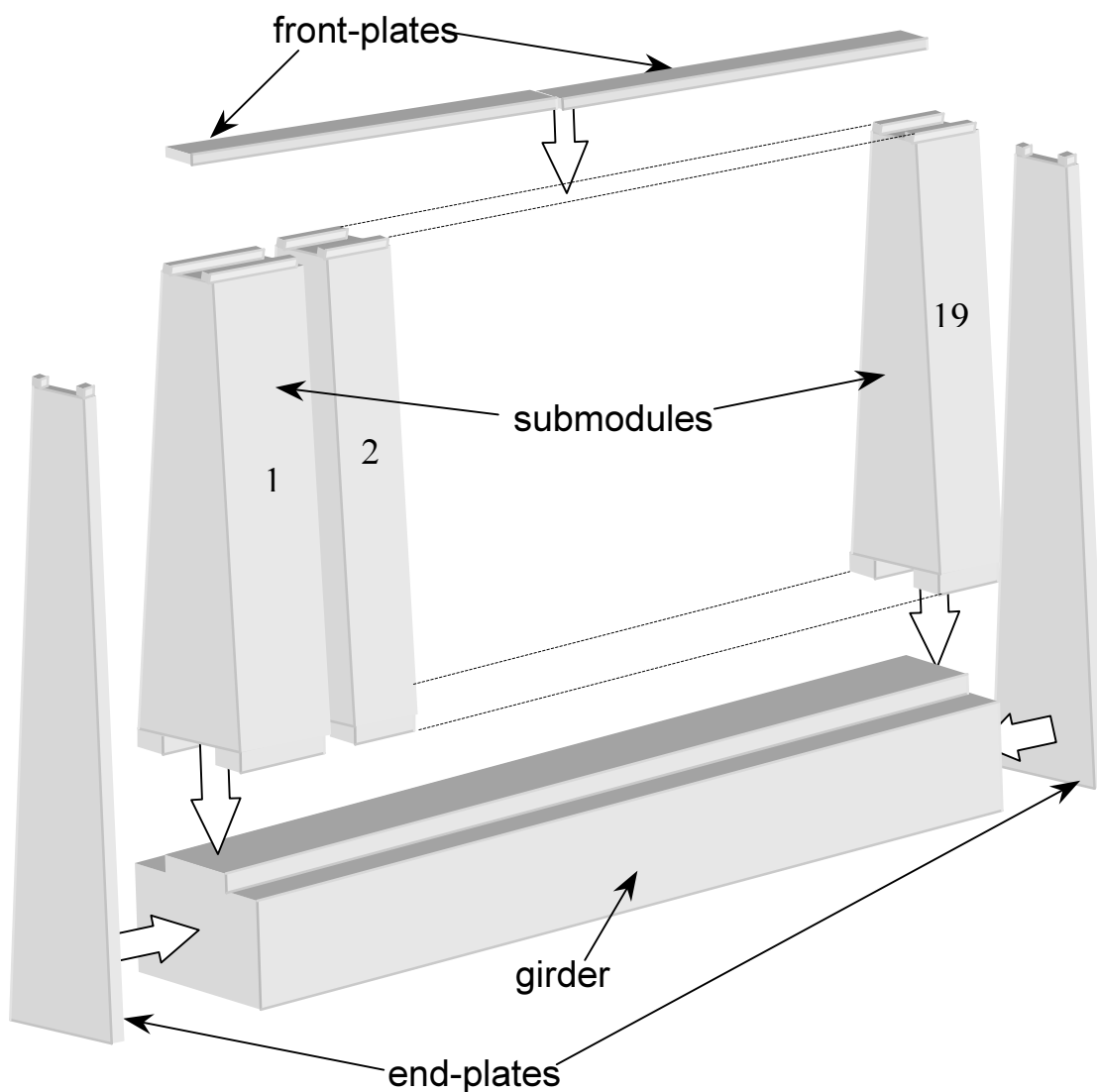
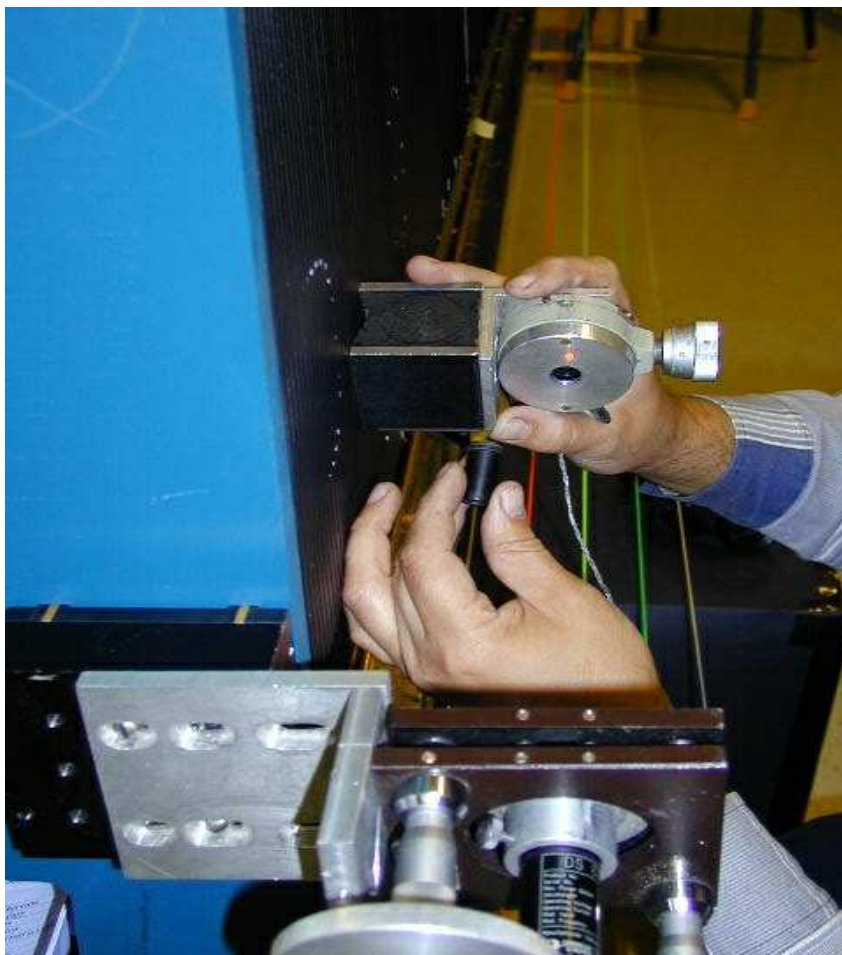


*Fig.13 Schematics of the MODULE assembly*

**LASER MEASUREMENT SYSTEM (LMS).**

Parts of the measurement equipment we use are precision instruments industrially produced: CALIPERS ( $\pm 20 \mu\text{m}$  precision) and MINILEVEL ( $\pm 10^{-5}$  rad/m precision).

The special Laser Measurement System we have designed and constructed has a potential of



precision of  $\pm 50 \mu\text{m}$  when operated over a distance of typically 6 m of length. The gaining factor has been in the combination of this precision to an operation and manipulation simplicity for this device.

The LMS has been designed and constructed for the control of the surface geometry. The LMS (Fig.14) consists of a laser and photo-detector (PhD) built up by 4 independent parts; both the laser and the PhD are fixed on special and high precision adjustment units.

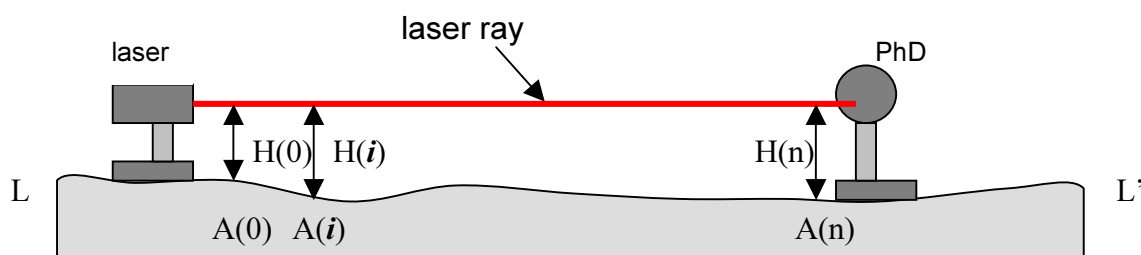


*Fig.14 LMS measuring principle.*

The LMS measurement principle was proposed by the authors for an earlier [2] application. Its principle is based on the measurements of the distance  $H(i)$  between the surface under control ( $LL'$ ) and the axis of the laser beam directed in a quasi-parallel way to that surface (Fig.14). By positioning the PhD detector at different positions  $A(i)$ , the associated values of  $H(i)$  are



determined by adjusting (using a system of a micro screws) the center of the photo detector relative to the laser beam. The full surface geometry is determined by a series of such measurements (Fig.15). The measurement precision is limited by the precision of the adjustment system and by the air convective

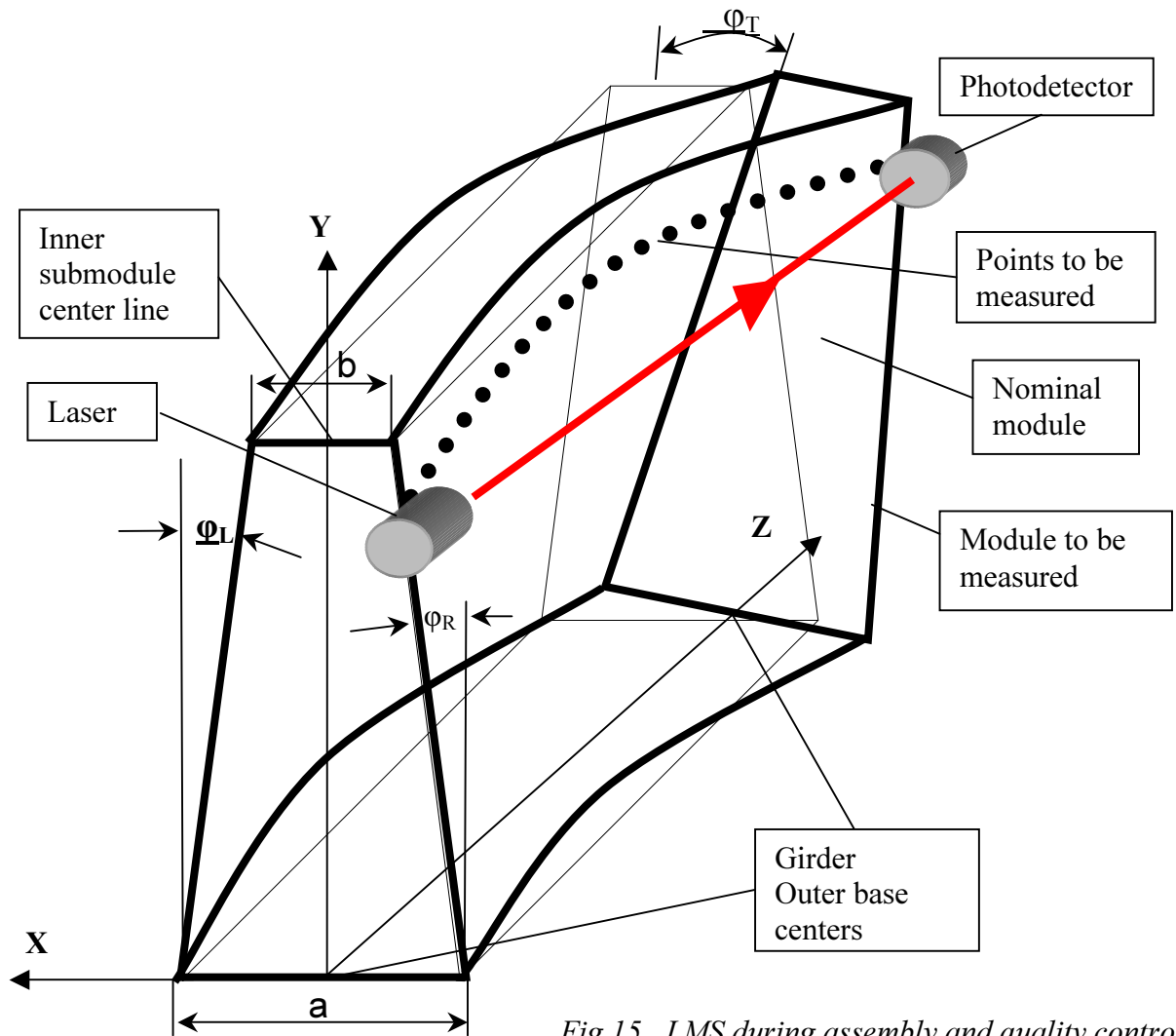
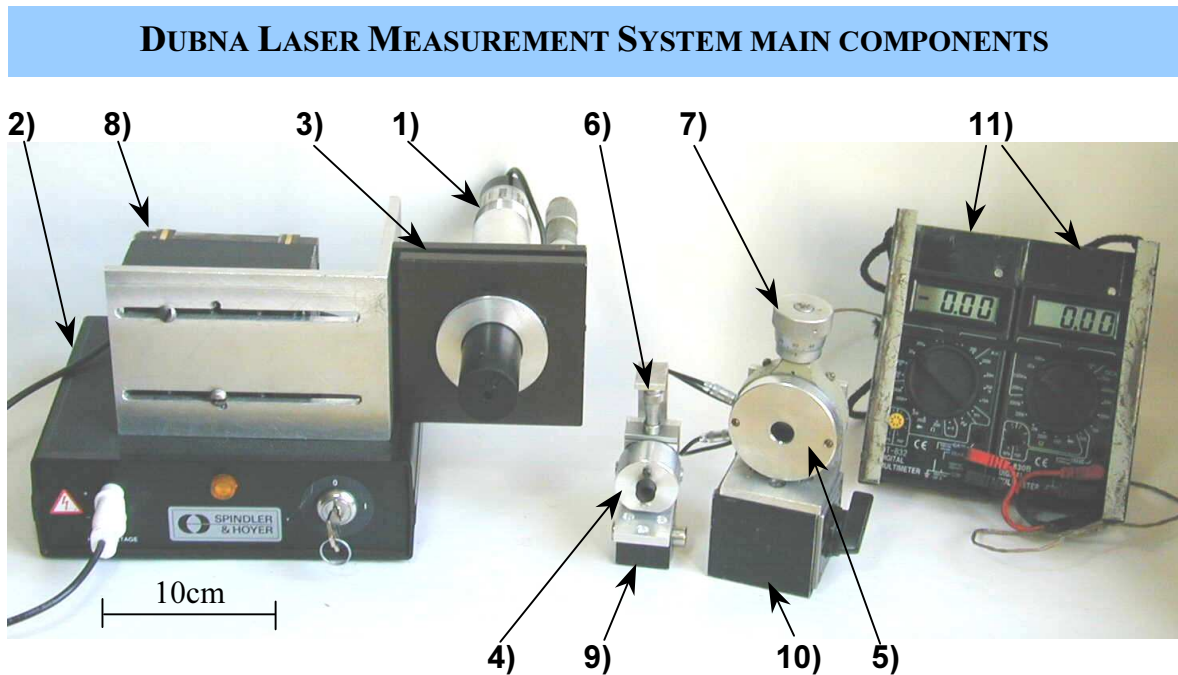


Fig.15 LMS during assembly and quality control

fluxes, which can be noticeably improved by positioning the laser beam inside a special telescopic dielectric tube.

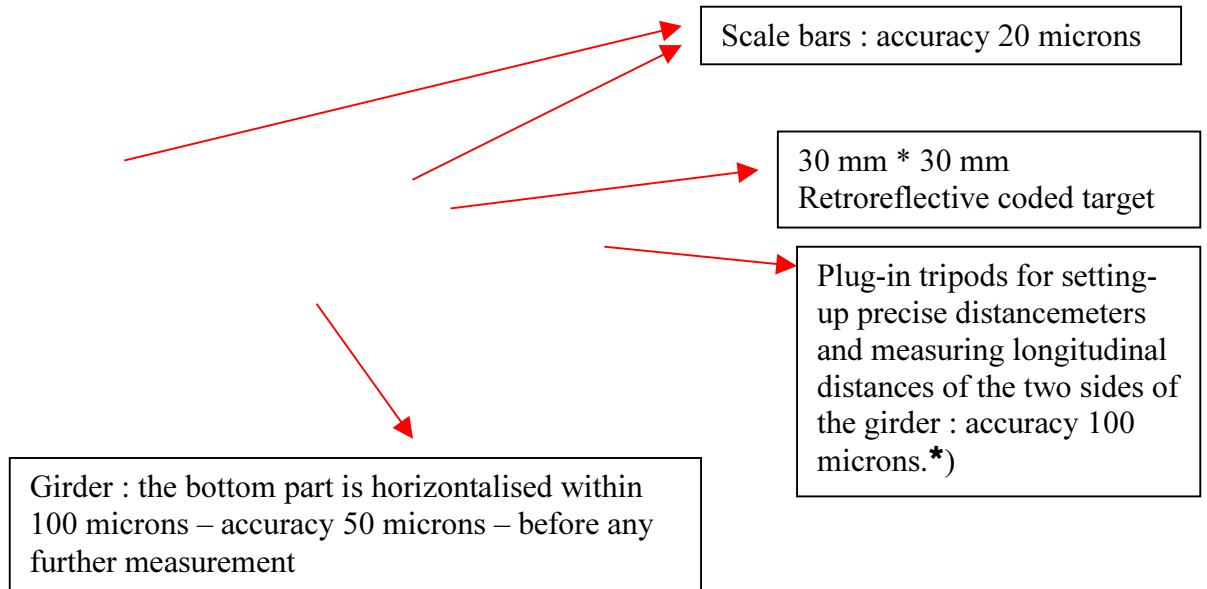
Multiple measurements done with our LMS have shown that the standard deviation value for individual H (n) measurements on a 6-m long calibrated base is 30  $\mu\text{m}$ . By adding to this the intrinsic precision the precision of the positioning of the LMS system on the surface to be measured (specific submodules surface), the resulting measurement precision for the entire area (1.9m x 5.6m) of the MODULE side surface is within  $\pm 50 \mu\text{m}$ .



- |                                    |     |
|------------------------------------|-----|
| <b>Laser</b>                       | 1)  |
| <b>Power module</b>                | 2)  |
| <b>Adjustment module</b>           | 3)  |
| <b>Quadrant photodiode devices</b> |     |
| Type I                             | 4)  |
| Type II                            | 5)  |
| <b>Positioning module</b>          |     |
| Type I                             | 6)  |
| Type II                            | 7)  |
| <b>Magnetic base</b>               |     |
| Type I                             | 8)  |
| Type II                            | 9)  |
| Type III                           | 10) |
| <b>Multimeters</b>                 | 11) |



**GEOMETRICAL AND PHOTOGRAMMETRIC OPERATIONS  
FOR THE MODULE#8**



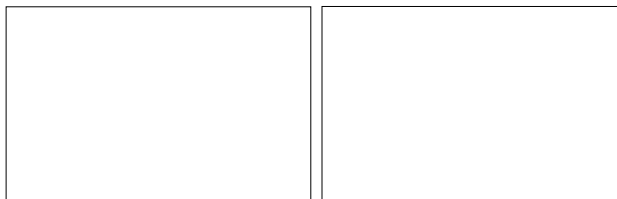
The MODULE#8 was measured at Cern in January 2000 first by theodolite – see the results in <http://edms.cern.ch/document/309991/1> – then by photogrammetry - see the results and the comparisons in <http://edms.cern.ch/document/309987/1>

\*) this tripod was also used for the first measurement by theodolite : specific targets were hold in the gap between two successive plates so that the target was referred to the average external surface of four successive plates apart the gap.

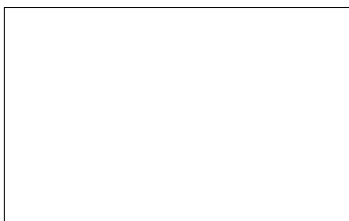
**CERN main photogrammetric equipment ...**



- DCS 460 - sensor CCD  $\Rightarrow$  6 millions pixels / pixel =  $9\mu\text{m}$
- 18 mm, 20 mm, 24 mm lenses
- Rollei DPA/CDW Software Package

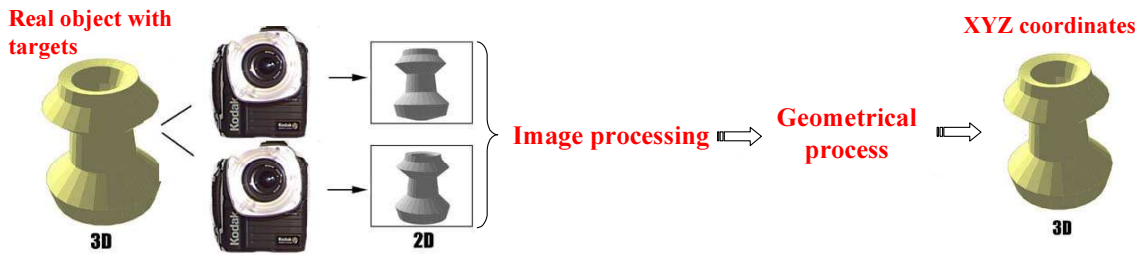


usual retro-reflective targets      strips and coded labels



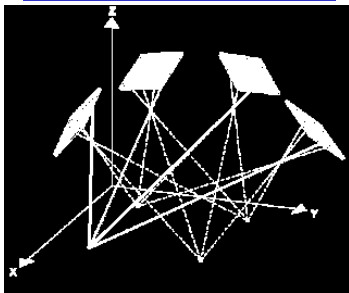
- f/16, f/22  $\Rightarrow$  under-exposed photos**
- $\Rightarrow$  necessity of reflective targets and annular flash
- $\Rightarrow$  good contrast
- $\Rightarrow$  image processing precision =  $1/30$  pixel =  $0.3\text{-}0.4\mu\text{m}$

**What is Digital Photogrammetry ?  
... 3-D coordinate measuring technique**



At least 2 images from 2 different locations. One not measure the object itself...but its image.

• GEOMETRICAL PROCESS :



1 - Multi-image orientation

**Resection** = process that enables to know the camera position and aiming angles

**Triangulation** = intersecting lines in space, computes the location of a point in all three dimensions

⇒ **Approximate positions and approximate coordinates**  
= 3 translations + 3 rotations

**What is Digital Photogrammetry ?  
... 3-D coordinate measuring technique**

2 -Perspective rays adjustment :

interior (image system - self calibration → systematic error camera) and exterior orientations (object system) of the camera adjusted together

• SCALING PHOTOGRAMMETRY :

Need to use calibrated scale bars and/or known distances on the object

**Forms ! Dimensions ?**

**Forms ! Dimensions !**

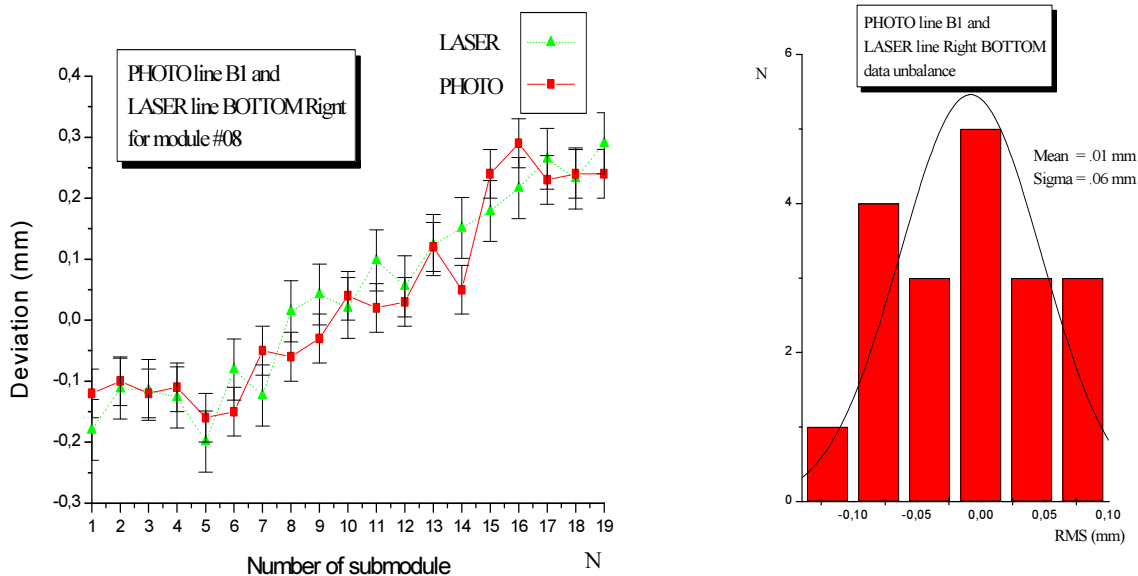
least squares ⇒ 3D object coordinates ⇒ statistical analysis ⇒ error budget...  
geometrical modeling... as built/reverse engineering ...

**DEVIATION OF THE MEASURED POINTS  
FROM THE SURFACE OF THE NOMINAL MODULE**

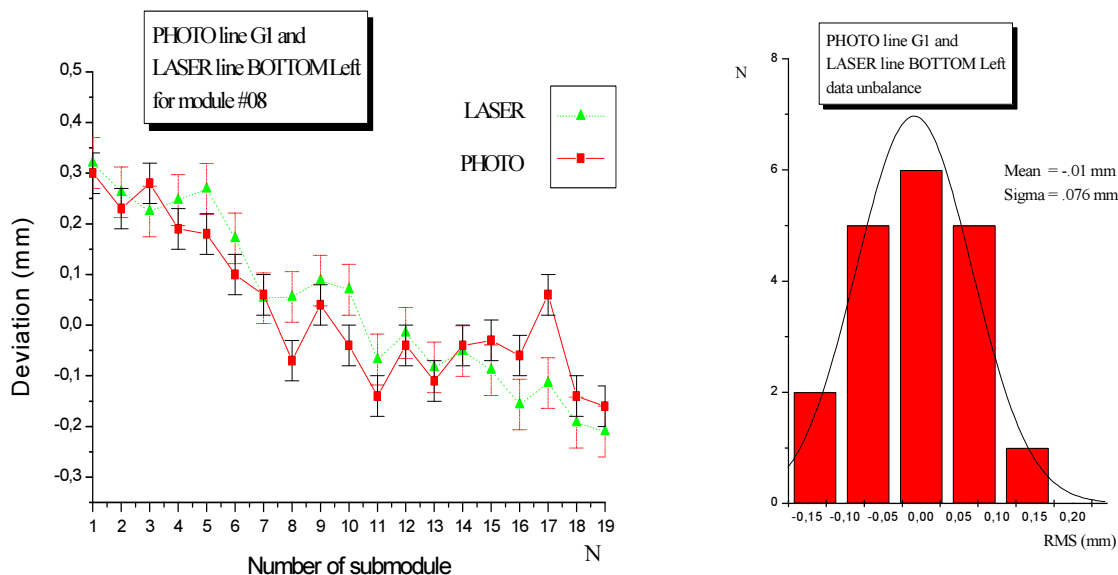
The results of the LASER (*BotR*, *TopR*, *TopL*, *BotL*) and PHOTOGRAMMETRY (*Bell*, *Bel4*, *Gex4*, *Gex1*) methods are presented in the form of the table of deviation of the measured points from the surface of the Nominal MODULE for each submodule. The left (right) side of the MODULE is the side on the left (right) of the observer looking from the SM1 along the MODULE

Right side				Number of sub- module	Left side			
Distances for BOTTOM line		Distances for TOP line			Distances for TOP line		Distances for BOTTOM line	
<i>Bell</i>	<i>BotR</i>	<i>Bel4</i>	<i>TopR</i>		<i>Gex4</i>	<i>TopL</i>	<i>Gex1</i>	<i>BotL</i>
-0.12	-0.18	0.04	-0.28	<b>1.</b>	0.22	-0.23	0.30	-0.18
-0.10	-0.14	0.11	-0.14	<b>2.</b>	0.13	-0.35	0.23	-0.21
-0.12	-0.17	0.17	0.06	<b>3.</b>	-0.10	-0.44	0.28	-0.22
-0.11	-0.21	0.14	-0.13	<b>4.</b>	-0.02	-0.33	0.19	-0.17
-0.16	-0.31	0.08	-0.34	<b>5.</b>	0.00	-0.22	0.18	-0.12
-0.15	-0.22	0.19	-0.22	<b>6.</b>	-0.11	-0.24	0.10	-0.19
-0.05	-0.29	0.21	-0.08	<b>7.</b>	-0.21	-0.44	0.06	-0.28
-0.06	-0.18	0.14	-0.11	<b>8.</b>	-0.10	-0.12	-0.07	-0.25
-0.03	-0.18	0.22	-0.16	<b>9.</b>	-0.12	-0.22	0.04	-0.19
0.04	-0.23	0.29	0.06	<b>10.</b>	-0.27	-0.26	-0.04	-0.18
0.02	-0.18	0.07	-0.32	<b>11.</b>	-0.16	-0.28	-0.14	-0.29
0.03	-0.25	0.12	-0.41	<b>12.</b>	0.06	-0.05	-0.04	-0.21
0.12	-0.21	0.08	-0.40	<b>13.</b>	0.00	-0.01	-0.11	-0.25
0.05	-0.21	-0.06	-0.54	<b>14.</b>	0.06	0.18	-0.04	-0.19
0.24	-0.21	-0.05	-0.49	<b>15.</b>	0.18	0.14	-0.03	-0.20
0.29	-0.20	-0.16	-0.70	<b>16.</b>	0.33	0.26	-0.06	-0.24
0.23	-0.18	-0.09	-0.58	<b>17.</b>	0.38	0.52	-0.06	-0.17
0.24	-0.24	-0.25	-0.86	<b>18.</b>	0.33	0.35	-0.14	-0.22
0.24	-0.21	-0.29	-0.96	<b>19.</b>	0.38	0.48	-0.16	-0.21

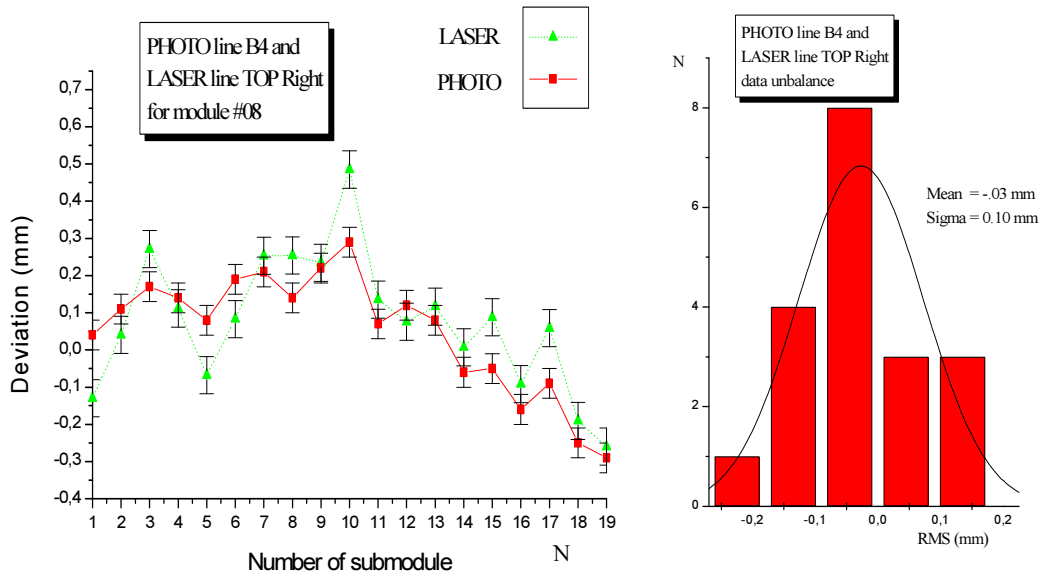
**RESULTS OF COMPARISON**



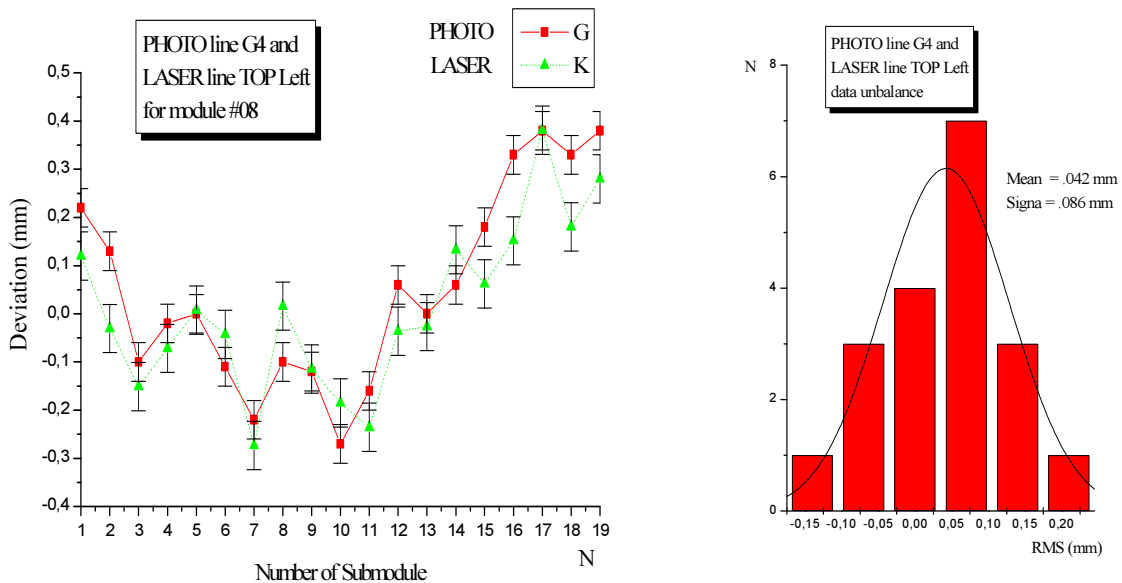
*Line Bell measurements data by the Photogrammetric and Laser Bottom-right methods after correction (turn by  $0.8 \times 10^{-4}$  rad)*



*Line Gex1 measurements data by the Photogrammetric and Laser Bottom-left methods after correction (turn by  $0.8 \times 10^{-4}$  rad)*



*Line Bel4 measurements data by the Photogrammetric and Laser Top-right methods after correction (turn by  $0.8 \times 10^{-4}$  rad)*



*Line Gex4 measurements data by the Photogrammetric and Laser Top-left methods after correction (turn by  $0.8 \times 10^{-4}$  rad)*